Early Use of Pressure Flaking on Lithic Artifacts at Blombos Cave, South Africa

Vincent Mourre *et al.*

Science **330**, 659 (2010);
DOI: 10.1126/science.1195550

Science (print ISSN 0036-8075; online ISSN 1095-9203) is published weekly, except the last week in December, by the American Association for the Advancement of Science, 1200 New York Avenue NW, Washington, DC 20005.

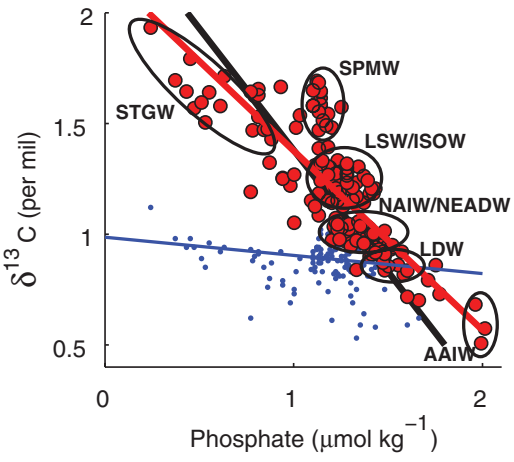

Fig. 2. Relationship between phosphate and $\delta^{13}C$ (blue) and $\delta^{13}C^{PI}$ (red) with linear regression lines as determined from samples obtained deeper than 200 m north of 20°N at the 1993 Malcolm Baldridge cruise. The black line is the –1.1 relationship expected in the absence of thermodynamic fractionation (*10*). Ellipses indicate typical $\delta^{13}C^{PI}$ and PO_4 values for the different water masses.

In addition to the LSW, other high-$\delta^{13}C^{PI}$ water masses such as Subpolar Mode Water (SPMW), Iceland Scotland Overflow Water (ISOW), and Subtropical Gyre Water (STGW) are also apparent. Indeed, accounting for the C-13 Suess effect strengthens the overall NA $\delta^{13}C$-versus-phosphate (PO_4) relationship (Fig. 2). Our preindustrial $\delta^{13}C$-PO_4 slope of –0.7‰ is essentially identical to the slope estimated through an independent approach (*9*) and close to the expected biological regression (*10*). Although there are still distinct thermodynamic isotopic signatures between southern and northern Atlantic water masses (i.e., warm STGW and cold SPMW are, respectively, depleted and enriched in $\delta^{13}C$ relative to their nutrient levels), our analysis reveals that the NA $\delta^{13}C$ is more strongly influenced by biological processes than previously appreciated.

Having defined the pristine NA $\delta^{13}C$ distribution allows us to better discern the similarities and differences between the modern and glacial oceans. NA $\delta^{13}C^{PI}$ shows notable similarities with reconstructed glacial NA $\delta^{13}C$. After correction, the SPMW end-member value (1.5 to 1.7‰) is about equal to that of the GNAIW of 1.5‰ (*3*). Thus, our reconstruction effectively removes at least one of the perceived differences between the glacial and present NA: the higher glacial northern end-member $\delta^{13}C$. Further, STGW samples have among the highest $\delta^{13}C^{PI}$ values found in our section (Fig. 2), suggesting that, just as proposed for the glacial ocean (*3*), elevated $\delta^{13}C$ in subtropical feed waters are important for achieving the high $\delta^{13}C$ of NA water masses (e.g., GNAIW). In summary, changes in water mass formation processes are not necessarily required to explain the high GNAIW end-member $\delta^{13}C$ values.

Despite these similarities, the glacial ocean was still distinct in a number of ways. The higher $\delta^{13}C$ values found in the modern deep (>2 km) NA ocean relative to glacial (*4*) cannot be a byproduct of the C-13 Suess effect. Likewise, if glacial water mass formation processes (end-member $\delta^{13}C$ values) were similar to today, other processes must be invoked to explain the geographic expansion of high $\delta^{13}C$ waters in the upper 2 km of the Atlantic (*4*). Taken together, our analysis emphasizes the role of water mass geometry and/or renewal rates (as opposed to end-member changes) in affecting glacial-interglacial $\delta^{13}C$ differences.

Our C-13 Suess effect correction elucidates the influence of individual components of NADW on ocean $\delta^{13}C$ and allows both rapid and large NA downcore $\delta^{13}C$ variability to be understood in the context of existing water masses. Comprehensive application of our C-13 Suess correction, for example, during the GEOTRACES program, would allow paleoceanographers to fully use the potential contained within the vast database of sedimentary $\delta^{13}C$ accumulated in recent decades. Ultimately, such a $\delta^{13}C^{PI}$ database is needed to provide accurate reference fields both for model evaluation and to achieve the improved proxy calibration and uncertainty estimates required to infer and quantify changes in past ocean circulation (*11*).

References and Notes

1. P. M. Kroopnick, *Deep-Sea Res.* **32**, 57 (1985).
2. D. W. Oppo, J. F. McManus, J. L. Cullen, *Nature* **422**, 277 (2003).
3. D. W. Oppo, S. J. Lehman, *Science* **259**, 1148 (1993).
4. W. B. Curry, D. W. Oppo, *Paleoceanography* **20**, PA1017 (2005).
5. C. Lyell, *The Principles of Geology* (Murray, London, 1830–1833).
6. P. D. Quay, B. Tilbrook, C. S. Wong, *Science* **256**, 74 (1992).
7. Information on material and methods, as well as water mass distribution, is available as supporting material on *Science* Online.
8. I. Yashayaev, A. Clarke, *Oceanography* **21**, 30 (2008).
9. R. Keir, G. Rehder, E. Suess, H. Erlenkeuser, *Global Biogeochem. Cycles* **12**, 467 (1998).
10. W. S. Broecker, E. Maier-Reimer, *Global Biogeochem. Cycles* **6**, 315 (1992).
11. O. Marchal, W. B. Curry, *J. Phys. Oceanogr.* **38**, 2014 (2008).

12. This work was supported by funding from the Norwegian Research Council (A-CARB) and contributes to EU-FP7 IP Past4Future. It is publication no. A305 from the Bjerknes Centre for Climate Research.

Supporting Online Material

www.sciencemag.org/cgi/content/full/330/6004/658/DC1
Materials and Methods
SOM Text
Figs. S1 and S2
References and Notes

15 June 2010; accepted 17 September 2010
10.1126/science.1193769

Early Use of Pressure Flaking on Lithic Artifacts at Blombos Cave, South Africa

Vincent Mourre,[1,2] Paola Villa,[3,4,5*] Christopher S. Henshilwood[6,7]

Pressure flaking has been considered to be an Upper Paleolithic innovation dating to ~20,000 years ago (20 ka). Replication experiments show that pressure flaking best explains the morphology of lithic artifacts recovered from the ~75-ka Middle Stone Age levels at Blombos Cave, South Africa. The technique was used during the final shaping of Still Bay bifacial points made on heat-treated silcrete. Application of this innovative technique allowed for a high degree of control during the detachment of individual flakes, resulting in thinner, narrower, and sharper tips on bifacial points. This technology may have been first invented and used sporadically in Africa before its later widespread adoption.

Pressure flaking is a retouching (*1*) technique used by prehistoric knappers to shape stone artifacts by exerting a pressure with the narrow end of a tool close to the edge of a worked piece. The earliest evidence of pressure flaking (*2*, *3*) was thought to come from the Upper Paleolithic Solutrean industry of Western Europe dating to ~20,000 years ago (20 ka) (*4*–*6*). In later times, it was used to produce Paleoindian projectile points (*7*), microlithic backed tools in the Later Stone Age of Africa (*8*), and bifacial arrowheads in the Holocene of North America and Australia (*9*, *10*). Retouch by pressure provides the flintknapper with a degree of control over the final shape, regularity, and thinness of the tool edge that cannot be achieved by direct percussion.

With the exception of obsidian, jasper, and some high-quality flint (*11*), few lithic materials

[1]INRAP Méditerranée, 561 rue Étienne Lenoir-KM Delta, 30900 Nîmes, France. [2]TRACES-UMR 5608, Université de Toulouse-Le Mirail, 31058 Toulouse, France. [3]University of Colorado Museum, Boulder, CO 80309–0265, USA. [4]Institut de Préhistoire et Géologie du Quaternaire, UMR 5199 PACEA, Université Bordeaux 1, 33405 Talence, France. [5]School of Geography and Environmental Studies, University of the Witwatersrand, Johannesburg, South Africa. [6]Institute for Archaeology, History, Culture and Religion, University of Bergen, Bergen, Norway. [7]Institute for Human Evolution, University of the Witwatersrand, Johannesburg, South Africa.

*To whom correspondence should be addressed. E-mail: villap@colorado.edu

can be pressure-flaked in their natural state, but heat treatment can improve the flaking quality of some of them (*12*). Early evidence for heat treatment of silcrete at ~164 ka comes from Pinnacle Point, southern Cape, South Africa (*13*).

Here, we show through experimental replication and microscopic study that silcrete artifacts from the ~75-ka Still Bay levels at Blombos Cave (*14*) (fig. S1) were also heat-treated before flaking and that pressure flaking was used during the final retouch phase of the Still Bay points. These bifacial points were axially hafted, and impact scars on recovered tools demonstrate that they were used as hunting weapons (*15*).

The manufacturing sequence of the Blombos Still Bay points can be divided into four production phases (*15*) (fig. S2). Direct percussion by hard hammer is used in the initial shaping (production phase 1). Advanced shaping is done by soft hammer marginal percussion (phase 2a with hard and soft hammer scars and phase 2b with only soft hammer scars). In the final phase (phase 3), retouch is applied to the edges, especially the tip. A small number of points were reworked by hard hammer percussion (phase 4). Here, we examine the finished products of production phase 3 and compare them with those from phase 2b.

Heat-treated silcrete can be recognized through the application of thermoluminescence and archeomagnetism, both destructive methods, and maximum gloss analysis that is nondestructive (*13*). We used a visual method commonly used to identify heat treatment on Paleoindian and Solutrean points [supporting online material (SOM)]. After the removal of a flake from unheated silcrete, the scar surface will have a rough, dull texture. If a silcrete piece had been heat-treated first, then the scar surface will have a smooth, glossy appearance. The contrast between the two surfaces is visible at low magnification (fig. S3). The visual method is based on contrast between the two types of surfaces; thus, it can be securely identified only on pieces where surfaces flaked before heating have not been completely removed by postheating intensive flaking (table S1). Because heating precedes the advanced flaking phases of the artifacts, it must have been a phase in the knapping process, before the final phase of retouch, and not accidental.

Different knapping techniques result in flake scar patterns with characteristic combinations of attributes (*16*–*18*). Experimental replication on the local raw material is essential to recognize the distinctive markers of different techniques. We collected silcrete from outcrops located ~30 km from Blombos Cave. Some were heat-treated following the method in (*13*). Blanks of unheated and heated silcrete were knapped with quartzite stone hammers and a wooden billet for the first phases of reduction. A bone flaker was used during the final pressure-retouching of the points.

Silcrete in its natural state can be flaked by hard hammer and can be trimmed by soft organic or soft stone hammer. However, during our experiments we found that the final phases of retouch (phase 3) observable on the Blombos bifacial points cannot be executed on unheated silcrete. For pressure flaking to be successful, the silcrete needs to be heat-treated. Regularity and parallelism of scars is considered the main trait of pressure flaking (*12*) (fig. S4). On flint, pressure will produce subparallel and rectilinear retouch scars with 10 to 15 mm of maximal length and up to 4 to 5 mm wide (*19*). However, the technical features described for flint are different from those observed on the Blombos bifacial points. It was on the basis of the flint features that we previously rejected the hypothesis of pressure retouch on the Blombos points (*15*).

Our experiments showed that wider flakes (up to 10 mm wide) can be detached by pressure retouch on heated silcrete and that the resultant scars are not always subparallel and rectilinear.

Table 1. Attributes of experimental flakes made by pressure and by marginal percussion with a soft hammer, compared to a sample of flakes from layer CC at Blombos. All flakes are ≤1 cm, to avoid differences that might be due to size.

Flake attributes	Experimental				Blombos layer CC	
	Pressure		Percussion by soft hammer			
	(*n* = 30)		(*n* = 30)		(*n* = 60)	
	n	%	*n*	%	*n*	%
Prominent bulb	28	93.3	4	13.3	21	35.0
Bulb without a lip	29	96.7	11	36.7	30	50.0
Small but not punctiform platform	29	96.7	24	80.0	49	81.7
Regular ridges	19	63.3	11	36.7	32	53.3
Hackles on the bulb	13	43.3	1	3.3	18	30.0

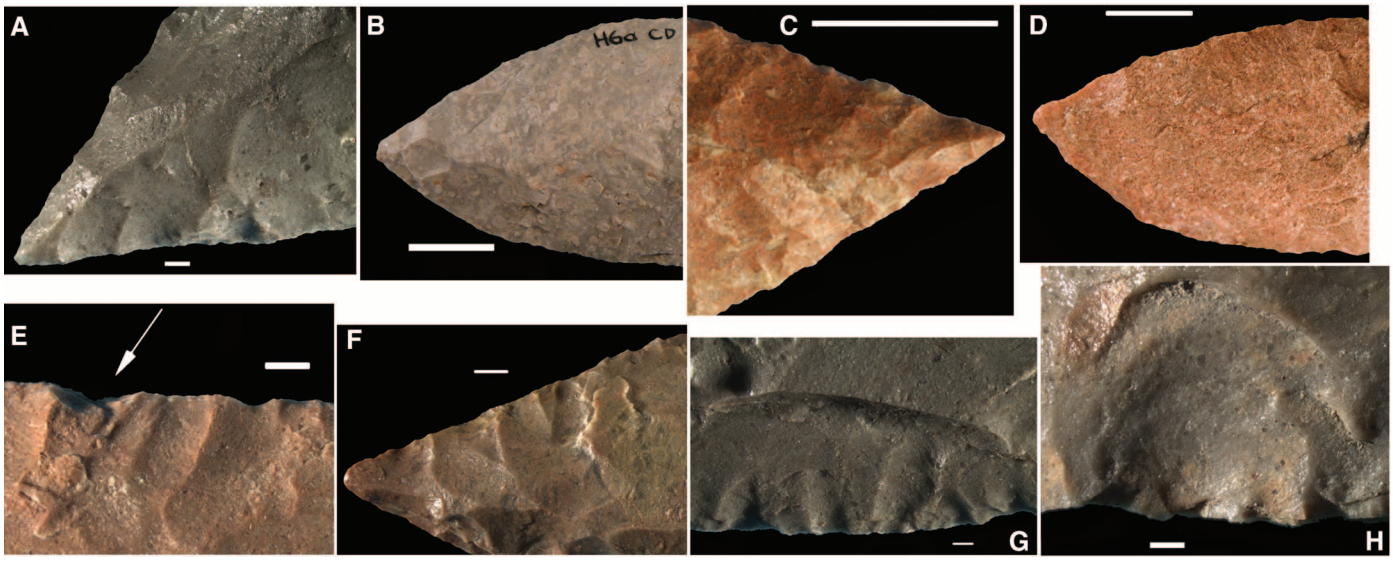

Fig. 1. Blombos Still Bay bifacial points, all production phase 3 except (D). (**A** to **D**) Examples of tip shapes; (**E** to **H**) examples of scar attributes diagnostic of pressure. (A) V-shaped tip with straight edges, PVN 45. (B) Arched tip with curved edges, PVN 66. (C) V-shaped tip with straight edges, P. 68. (D) Tip with irregular, asymmetrical sides, PVN 27, phase 2b. (E) Hackles (white arrow) on the bulb negative, PVN 84. (F) Regular ridges, PVN 68. (G) Pressure scars with deep bulb negatives inside a larger scar by direct percussion, PVN 45. (H) Deep bulb negative, Mus.2. Scale bars: (A, E to H), 1 mm; (B to D), 1 cm.

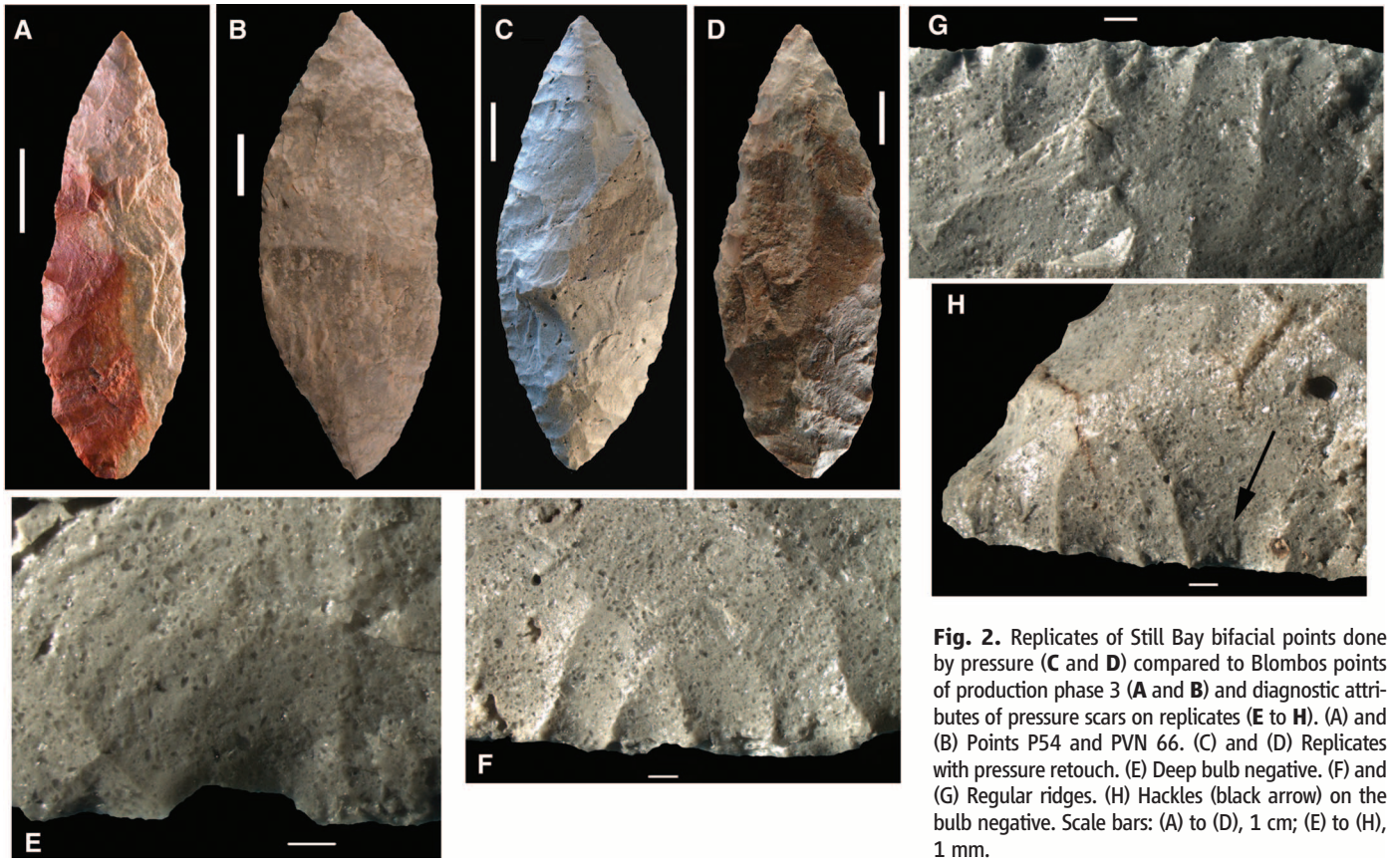

Fig. 2. Replicates of Still Bay bifacial points done by pressure (**C** and **D**) compared to Blombos points of production phase 3 (**A** and **B**) and diagnostic attributes of pressure scars on replicates (**E** to **H**). (A) and (B) Points P54 and PVN 66. (C) and (D) Replicates with pressure retouch. (E) Deep bulb negative. (F) and (G) Regular ridges. (H) Hackles (black arrow) on the bulb negative. Scale bars: (A) to (D), 1 cm; (E) to (H), 1 mm.

Table 2. Frequencies of attributes for the identification of flaking techniques and tip measurements of the Blombos Still Bay points compared to unifacial points from the post-Howiesons Poort of Sibudu (database of P. Villa).

Attributes	Phase 2b		Phase 3	
	n	%	*n*	%
Scar width ≤10 mm	24/50	48.0	55/55	100
Deep bulb negative	10/24	41.7	50/55	90.9
Regular ridges	7/24	29.2	43/55	78.2
V-shaped tip with straight edges	0/15	0	21/43	48.8
Hackles on the bulb negative	0/24	0	17/55	30.9

Tip angle (degrees)	Mean	SD	*n*
Phase 3 points			
V-shaped tip with straight edges	51.2	6.8	21
Arched tip with curved edges	63.2	6.5	20
Phase 2b points			
Tip with irregular or asymmetrical edges	65.4	7.0	11
Unifacial points from post-Howiesons Poort (HP) layers at Sibudu (RSp-MOD ~47 ka)	65.9	11.1	83

Tip thickness (mm)	Mean	SD	N
Phase 3 points	3.7	0.7	44
Phase 2b points	4.5	1.0	11
Unifacial points from post-HP layers at Sibudu (RSp-MOD ~47 ka)	5	1.4	84

Our analysis also provided a number of criteria to distinguish between pressure and soft hammer flaking (Table 1, Figs. 1 and 2, and figs. S5 to S7). Three of the attributes in Table 1 (a prominent bulb, no lip on the bulb, and hackles on the bulb) occurred in high proportions on pressure flakes, in contrast to flakes made by soft hammer. χ^2 values are high ($P < 0.001$ in all cases; SOM). Two other features (small platforms and regular ridges) seem less useful for discriminating between the two techniques. Intermediate frequency values in the Blombos flake sample show that both techniques were used by the tool makers.

The distinctiveness of the two flaking modes is also seen in the frequency distribution of scar dimensions (table S2). The mean width and length of scars on Blombos production phase 3 points are similar to those of experimental scars by pressure, whereas the scars of phase 2b points are more similar to the scars of our experimental soft hammer percussion points. To identify the flaking technique used on the Blombos bifacial points, we calculated the frequencies of five attributes (Table 2). Four of these were observed on experimental pressure scars and flakes (deep bulb negative, hackles on the bulb negative, scars ≤10 mm, and regular ridges; Figs. 1 and 2). Another attribute (V-shaped tips with straight edges) is based on expectations of rectilinear edges made by pressure (fig. S4, E and F). Two attributes, V-shaped tips with straight edges and hackles on the bulb negative, do not occur at all on phase 2b points made by soft hammer. Thus, those two features discriminate between the two techniques. On phase 3 points, these features are consistently associated with two other distinctive attributes (deep bulb negative and regular ridges). We conclude that at least half of the production phase 3 points were

finished with the pressure technique to make the tip sides straight and regular.

The penetrating angle and tip thickness of phase 3 points are significantly smaller than those of phase 2b, inferred to have been made by direct percussion. They are also smaller than the tip angle and thickness of unifacial points produced on flakes retouched by direct percussion during post-Howiesons Poort to final Middle Stone Age (MSA) times in South Africa, ~58 to 40 ka, (*20*, *21*). T tests for tip angle and tip thickness of phase 3, 2b, and unifacial points show that differences between all three samples are significant (SOM). These differences confirm the advantages of using the pressure technique to obtain points with thinner, V-shaped tips with straight edges.

There are no known antecedents to the intensively flaked Still Bay bifacial points from Blombos, or evidence for earlier pressure flaking, in the MSA (*22*). After 72 ka, bifacial technology disappears in South Africa and is replaced after 65 ka by Howiesons Poort–type backed tools (*23*). Pressure flaking adds to the repertoire of technological advances during the Still Bay (*24*–*26*) and helps define it as a time when novel ideas and techniques were rapidly introduced. This flexible approach to technology may have conferred an advantage to the groups of *Homo sapiens* who migrated out of Africa after ~60 ka (*27*).

References and Notes

1. The use of pressure to remove blades and bladelets from a core is a more complex technique that appears in Northern Asia at about 25 ka (*12*).
2. Possible evidence of heat treatment and pressure retouch has been suggested (*3*) for the Early Upper Paleolithic Streletskayan bifacial points of Kostienki 1.
3. B. A. Bradley, M. Anikovich, E. Giria, *Antiquity* **69**, 989 (1995).
4. M. Tiffagom, *Paléo* **10**, 147 (1998).
5. T. Aubry, B. Walter, E. Robin, H. Plisson, M. Ben-Habdelhadi, *Paléo* **10**, 163 (1998).
6. M.-L. Inizan, J. Tixier, *Paléorient* **26**, 23 (2001).
7. F. Sellet, *J. Archaeol. Sci.* **31**, 1553 (2004).
8. C. B. Bousman, *J. Anthropol. Archaeol.* **24**, 193 (2005).
9. G. C. Frison, *Prehistoric Hunters of the High Plains* (Academic Press, San Diego, 1991).
10. R. Harrison, *Archaeol. Oceania* **39**, 1 (2004).
11. D. E. Crabtree, *Tebiwa* **10**, 8 (1967).
12. M.-L. Inizan, M. Reduron-Ballinger, H. Roche, J. Tixier, *Technology and Terminology of Flaked Stone* (CREP, Nanterre, 1999).
13. K. S. Brown *et al.*, *Science* **325**, 859 (2009).
14. Z. Jacobs, G. A. T. Duller, A. G. Wintle, C. S. Henshilwood, *J. Hum. Evol.* **51**, 255 (2006).
15. P. Villa, M. Soressi, C. S. Henshilwood, V. Mourre, *J. Archaeol. Sci.* **36**, 441 (2009).
16. K. Ohnuma, C. Bergman, *Bull. Inst. Arch. London* **19**, 161 (1982).
17. J. Pelegrin, in *L'Europe centrale et septentrionale au Tardiglaciaire*, B. Valentin, P. Bodu, M. Christensen, Eds. (Mémoire du Musée de Préhistoire d'Ile-de-France 7, Nemours, 2000), pp. 73–86.
18. S. Soriano, P. Villa, L. Wadley, *J. Archaeol. Sci.* **34**, 681 (2007).
19. H. Plisson, J.-M. Geneste, *Paléo* **1**, 65 (1989).
20. Z. Jacobs, A. G. Wintle, G. A. T. Duller, R. G. Roberts, L. Wadley, *J. Archaeol. Sci.* **35**, 1790 (2008).
21. P. Villa, M. Lenoir, *Southern African Humanities* **18**, 89 (2006).
22. R. Singer, J. Wymer, *The Middle Stone Age at Klasies River Mouth in South Africa* (Chicago Univ. Press, Chicago, 1982).
23. P. Villa, S. Soriano, N. Teyssandier, S. Wurz, *J. Archaeol. Sci.* **37**, 630 (2010).
24. C. S. Henshilwood, F. d'Errico, I. Watts, *J. Hum. Evol.* **57**, 27 (2009).
25. F. d'Errico, C. S. Henshilwood, *J. Hum. Evol.* **52**, 142 (2007).
26. C. S. Henshilwood, F. d'Errico, M. Vanhaeren, K. van Niekerk, Z. Jacobs, *Science* **304**, 404 (2004).
27. H. Liu, F. Prugnolle, A. Manica, F. Balloux, *Am. J. Hum. Genet.* **79**, 230 (2006).

28. This research was funded by the Wenner-Gren Foundation (grant to P.V.). V.M.'s work was facilitated by a research convention between Inrap and the University of the Witwatersrand. Financial support was provided to C.S.H. by a European Research Council Advanced Grant TRACSYMBOLS (FP7 No. 249587); by a National Research Foundation/Department of Science and Technology–funded Chair at the University of the Witwatersrand, South Africa; by a Norwegian Research Council Grant; and by a PROTEA French–South Africa exchange program. We thank K. Brown for sharing information about silcrete heating and helping us in the experiments. V.M. thanks N. Schlanger for assistance. The Iziko Museum in Cape Town provided space and working facilities.

Supporting Online Materials

www.sciencemag.org/cgi/content/full/330/6004/659/DC1
Materials and Methods
Figs. S1 to S7
Tables S1 and S2
References

23 July 2010; accepted 16 September 2010
10.1126/science.1195550

Fitness Correlates of Heritable Variation in Antibody Responsiveness in a Wild Mammal

Andrea L. Graham,[1,2,3,4]* Adam D. Hayward,[2] Kathryn A. Watt,[2,3] Jill G. Pilkington,[2] Josephine M. Pemberton,[2] Daniel H. Nussey[2,4]

A functional immune system is important for survival in natural environments, where individuals are frequently exposed to parasites. Yet strong immune responses may have fitness costs if they deplete limited energetic resources or cause autoimmune disease. We have found associations between fitness and heritable self-reactive antibody responsiveness in a wild population of Soay sheep. The occurrence of self-reactive antibodies correlated with overall antibody responsiveness and was associated with reduced reproduction in adults of both sexes. However, in females, the presence of self-reactive antibodies was positively associated with adult survival during harsh winters. Our results highlight the complex effects of natural selection on immune responsiveness and suggest that fitness trade-offs may maintain immunoheterogeneity, including genetic variation in autoimmune susceptibility.

Immune systems of different individuals are notoriously heterogeneous in the strength, specificity, and efficacy of responses to infection, and much of the variation is under genetic control (*1*, *2*). Individuals likewise vary in their genetic susceptibility to generate self-targeted immune responses (autoimmunity) (*3*–*7*). The challenge is to explain why natural selection has failed to eliminate alleles that confer susceptibility to infection (*2*) or promote autoimmunity (*8*). One hypothesis is that individuals with strong immune responses experience fitness benefits of immunity (e.g., clearance of infection to promote survival or provision of maternal antibodies to promote offspring survival) but are also likely to suffer its costs (e.g., energetic drain and/or autoimmune disease) (*9*, *10*). Although wild rodents have autoimmune susceptibility genes (*3*) and higher standing antibody concentrations than their laboratory counterparts (*11*), autoimmunity is known only in people and laboratory, domestic, or captive mammals (*7*, *8*, *12*–*14*). Here, we assess the associations among antibody responses, survival, and traits associated with reproductive success in the wild.

The unmanaged population of Soay sheep (*Ovis aries*) in Village Bay, Hirta, St. Kilda, has been monitored since 1985, yielding detailed longitudinal information on both individual life histories and population dynamics (*15*). Using blood plasma samples collected during August of 11 years (1997 to 2007), we measured the concentration of antibodies that bind mammalian nuclear and cytoplasmic antigens (hereafter, antinuclear antibodies, or ANAs) (*12*, *16*, *17*). High concentrations of ANAs are indicative of high rates of division and antibody production by B and plasma cells (*18*), particularly in response to self-antigens (*6*). It is important to note that self-reactivity can represent a side effect of normal immune function (*19*, *20*). For example, although ANAs are potential markers of autoimmunity, they are also associated with useful defense mechanisms, such as natural antibodies (*20*). Only if ANAs are sustained at high titers, in combination with other markers, are they associated with autoimmune diseases like systemic lupus erythematosus in people and dogs (*12*, *16*).

ANAs were detectable in wild sheep at a prevalence comparable to that in human populations (*21*–*23*). We assayed 2622 plasma samples collected from 1476 sheep, so individual sheep were sampled 1.8 times, on average. We

[1]Department of Ecology and Evolutionary Biology, Princeton University, Princeton, NJ 08544, USA. [2]Institute of Evolutionary Biology, University of Edinburgh, Edinburgh EH9 3JT, Scotland. [3]Institute of Immunology and Infection Research, University of Edinburgh, Edinburgh EH9 3JT, Scotland. [4]Centre for Immunity, Infection and Evolution, School of Biological Sciences, University of Edinburgh, Edinburgh EH9 3JT, Scotland.

*To whom correspondence should be addressed. E-mail: algraham@princeton.edu